Proceedings from the Fourth International Conference on Advances in Materials Technology for Fossil Power Plants, October 25–28, 2004, Hilton Head Island, South Carolina.

DEGRADATION PROCESSES IN CREEP OF 9-12%Cr FERRITIC STEELS

V. Sklenicka
K. Kucharova
L. Kloc
M. Svoboda
Institute of Physics of Materials
Academy of Sciences of the Czech Republic
Zizkova 22
CZ-616 62 Brno, Czech Republic
J. Kudrman
UJP PRAHA a.s.
Nad Kaminkou 1345
CZ-156 10 Prague 5 – Zbraslav, Czech Republic

Abstract

Creep behavior and degradation of creep properties of advanced 9-12%Cr ferritic steels are phenomena of major practical relevance, often limiting the lives of power plant components and structures designed to operate for long periods under stress at elevated temperatures. Because life expectancy is, in reality, based on the ability of the material to retain its high-temperature creep strength for a period of at least twice the projected design life, methods of creep property assessment based on physical changes in the material that are likely to occur during service exposure rather than simple parametric extrapolation of the short-term data are necessary. This work attempts to highlight the problem areas just in this respect. The proposed approaches are illustrated by recent experimental results on advanced high creep strength 9-12%Cr ferritic-martensitic steels (P91 and P92).

Introduction

The long-term creep data required for design of large-scale components and structures for power stations are usually derived by extrapolation of short-term stress-rupture properties. Unfortunately, the short-term data for 9-12%Cr steels are characterized by a wide scatter band which arises from uncertainties of testing methods, material inhomogenities and microstructural instabilities. The influence of microstructural variability on creep properties is mechanism dependent, therefore, evaluation of the scatter caused by microstructural changes is only possible if the precise creep mechanisms of the material are known.

The present investigation was conducted on two modified 9-12%Cr steels (P91 and P92) in an effort to obtain more complete description and understanding of the role of degradation processes in high temperature creep. In order to accelerate some microstructural changes and thus to simulate long-term service conditions, isothermal aging at 1202°F (650°C) for 10000 h was applied to both steels in the as-received states. The standard tensile creep tests and the creep tests using of helicoids spring specimens were performed at 1112°F (600°C) on both the steels in the as-received state and after long-term isothermal aging.

Although the development and evaluation of 9-12%Cr steels have proceeded on the basis of simply laboratory–type tests, it is widely recognized that the realistic application of these materials is under conditions far different from those for which they were developed. When applied in service, the material is likely to be subjected to periodic removals of load, temperature, or both. Periodic applications of excessive loads and temperatures normally absent when the steel is evaluated. Thus the further object of the present paper is to attempt to obtain some information on the effects of nonsteady stressing and heating on the creep properties of P91 and P92 steels.

Experimental materials and procedures

The tempered martensite ferritic steel P91 (produced by Vitkovice Steel, Czech Republic) with the following chemical composition (in wt%) 0.09C, 0.56Mn, 0.20Si, 0.021P, 0.009S, 0.05Cu, 0.46Ni, 8.36Cr, 0.86Mo, 0.20V, 0.06Nb, 0.065N and 0.007Al was subjected to the two stage heat treatment: 1940°F (1060°C)/1h/air + 1382°F (750°C)/2h/air. The P92 material was received in the form of a seamless pipe produced by Nippon Steel Corporation with the following bulk chemical analysis (in wt%): 0.08C, 9.0Cr, 0.5Mo, 1.8W, 0.2V, 0.06Nb, 0.05N, 0.003B, <0.04Al with the following heat treatment: 1949°F (1065°C)/2h/air + 1418°F (770°C)/2h/air. Both P91 and P92 steels were investigated in as-received state (i.e. after heat treatment) and after isothermal annealing at 1202°F (650°C) up to 10000 hours.

Standard constant load tensile creep tests were carried out at temperature of 1112°F (600°C) with the testing temperature continuously monitored and maintained constant to within ± 0.5°C from the desired value [1]. The applied stresses ranged from 14500 to 50750 psi (100 to 350 MPa). The creep elongations were measured using a linear variable differential transducer (the strain was measured with a sensitivity of 5×10^{-6}) and they were continuously recorded digitally and computer processed. Short-term creep tests were performed on the P91 steel at temperature of 1112°F (600°C) and at stresses below 14500 psi (100 MPa) by means of the helicoid spring specimens technique [2]. Optical measurements of individual coil spacings were performed periodically and the creep strains were derived. Since the stress and strain in helicoid spring are essentially shear ones, they were transformed to the equivalent tensile quantities using a known relations $\sigma = \sqrt{3}\tau$ and $\varepsilon = \gamma\sqrt{3}$, where σ is tensile stress, τ is shear stress, ε is tensile strain and γ is shear strain.

The effect of temperature variation during the tensile creep exposure has been investigated by intermittent heating cycles in which the creep specimen was alternately held at a creep testing and room temperature for predetermined periods of time (~ 24 h at RT and ~ 144 h at 1112°F (600°C), respectively). In all cases the load was maintained constant during entire test.

Stress change creep experiments were carried out on the P91 steel at loading conditions corresponding to the low stress creep regime using the modified helicoid spring specimen technique [2]. All creep tests were conducted at the temperature of 1112°F (600°C) and applied stresses in the range of 5075 – 6380 psi (35 - 44 MPa).

The effect of long-term isothermal aging on the creep behavior of P91 and P92 steels

Creep results

Figures 1 and 2 show selected creep curves for steel P91 and steel P92 for uniaxial tensile creep tests conducted at 1112°F (600°C) under comparable levels of the applied stress σ. As demonstrated by the figures, significant differences were found in the creep behaviour of both steels in the as-received state when compared to their after aging state. First, the standard ε vs. t curves (Figs. 1 and 2) appear to show the long-term isothermal aging of the steels leads to an increase in the creep plasticity, which is proved in particular by the values of the total strains to fracture for the aged steels crept at low stresses (Figs. 1a and 2a). Second, the aged steels exhibit markedly shorter time to fracture than the steels in the as-received state over the entire stress range used. Third, the shapes of creep curves for both the as-received state and aged state of the steels differ considerably.

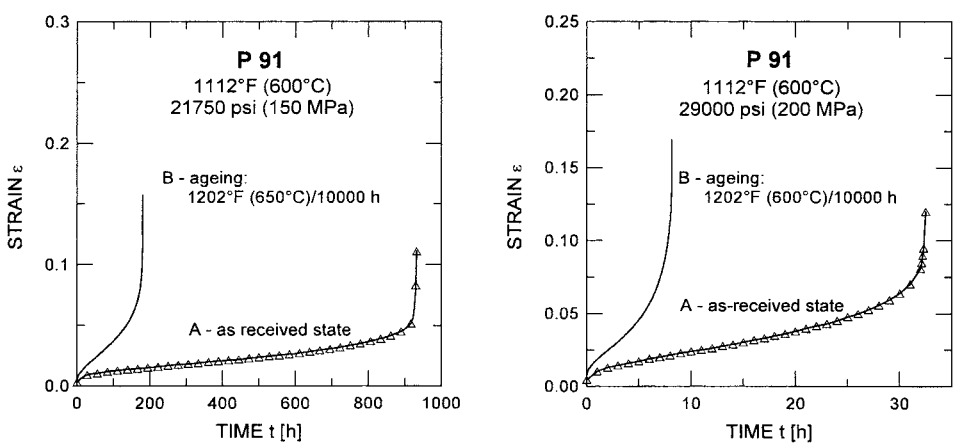

Figure 1. Creep curves of the P91 type steel in states A and B at 1112°F and two levels of applied stress: (a) 21750 psi and (b) 29000 psi

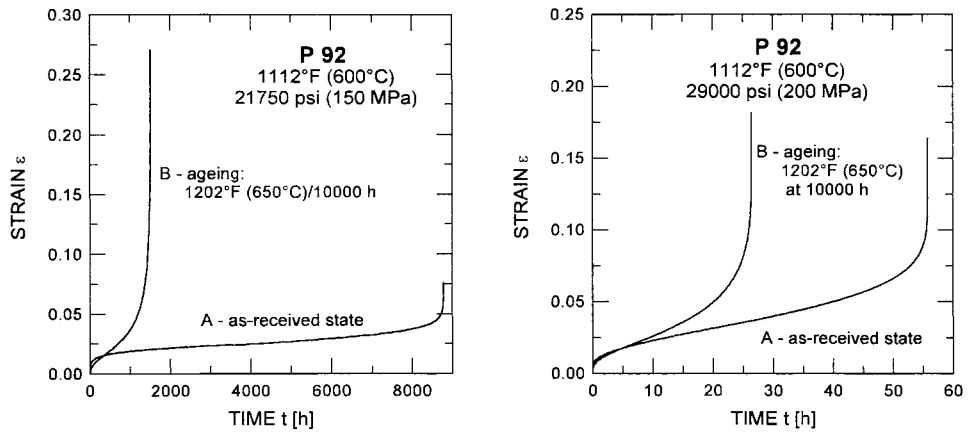

Figure 2. Creep curves of the P92 type steel in states A and B at 1112°F and two levels of applied stress: (a) 21750 psi and (b) 29000 psi

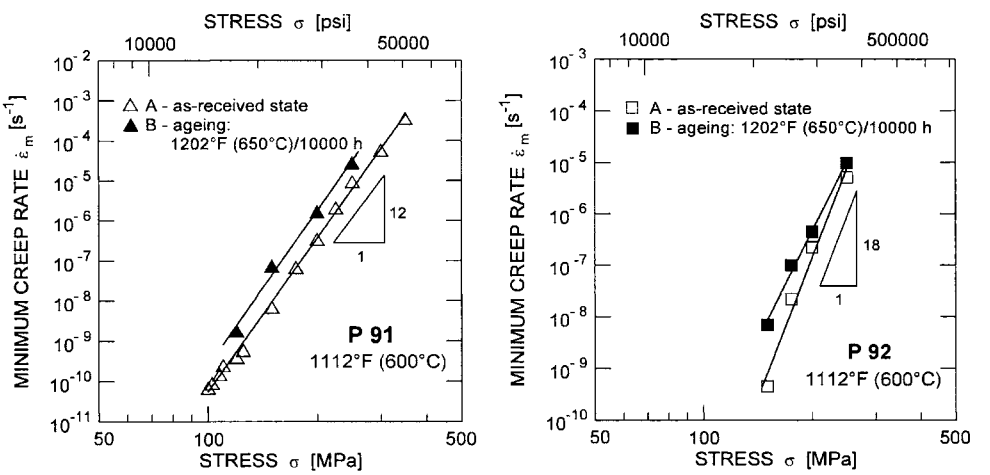

Figure 3. Stress dependence of minimum creep rate for (a) P91 and (b) P92 steels

In Fig. 3a,b the minimum creep rates $\dot{\varepsilon}_m$ are plotted against the applied stress σ on a logarithmic scale. Inspection of Fig. 3 leads to two observations. First, the steels in the as-received state exhibit better creep resistance than those after long-term ageing over the entire stress range used; the minimum creep for steel P91 in the as-received state is about order of magnitude less than that of the aged P91 steel. The stress dependences of the minimum creep rates for steel P92 are different in trend. While the slope and therefore the apparent stress exponents of creep rate

$n = (\partial \ln \dot{\varepsilon} / \partial \ln \sigma)_T$ are the same for steel P91 (Fig. 3a) the slope and the stress exponent n for steel P92 depends on its state; the difference for the state after ageing increases with decreasing applied stress (Fig. 3b). For both steels, the double logarithmic plots of the time to fracture t_f as a function of applied stress are shown in Fig. 4. It is clear from these plots that the creep life of steels in the as-received state is longer than in aged steels. While the difference for steel P91 is independent of applied stress (Fig. 4a) for steel P92, this difference consistently decreases with increasing applied stress, with a tendency at the higher stresses towards no effect of the state of steel on the lifetime.

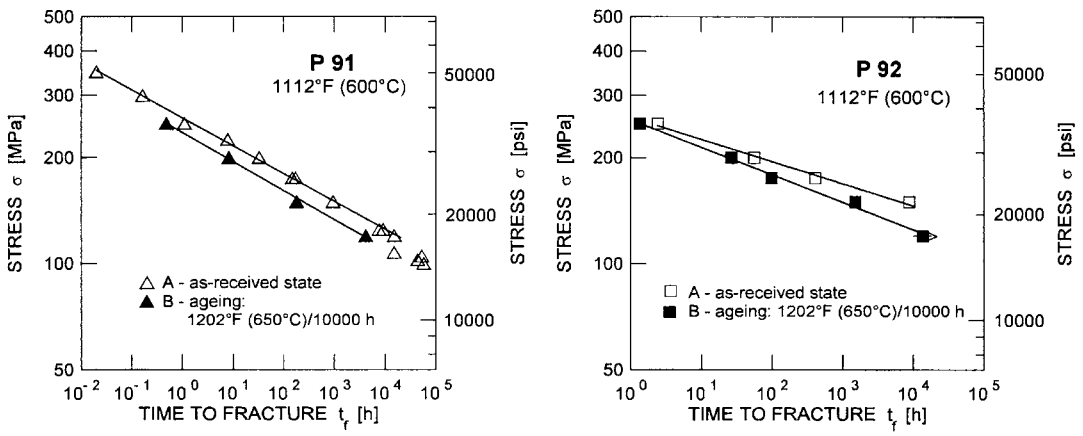

Figure 4. Stress dependence of time to fracture for (a) P91 and (b) P92 steels

Creep testing by means of the helicoid spring specimens was performed at the applied stress ranging from 145 to 14500 psi (1 to 100 MPa) and at 1112°F (600°C) on steel P91 in both the as-received and aged states. The minimum creep rates $\dot{\varepsilon}_{min}$ ranging from 8×10^{-4} to 1×10^{-12} s^{-1} correspond to these loading conditions – Fig. 5. Inspection of this figure suggests that the minimum creep rates are proportional to applied stress up to about 14500 psi (100 MPa), i.e. $n \cong 1$. Mutual comparison of the creep results obtained by the helicoid spring specimen technique with the results of standard uniaxial tensile creep tests on the steel investigated has shown very good coherency of both creep testing techniques. The transition from power-law creep (dislocation creep) with the stress exponent of the creep rate n of about 12 to the viscous creep (n = 1) was found at stresses around 14500 psi (100 MPa) at 1112°F (600°C) – Fig. 5. It should be stressed that any extrapolation from the power-law creep regime to stress below 14500 psi (100 MPa) may lead to serious underestimation of the creep rate predicted. No substantial effect of long-term ageing was found for the viscous creep. The creep rate for the aged state seems to be slightly lower than those for the as-received state.

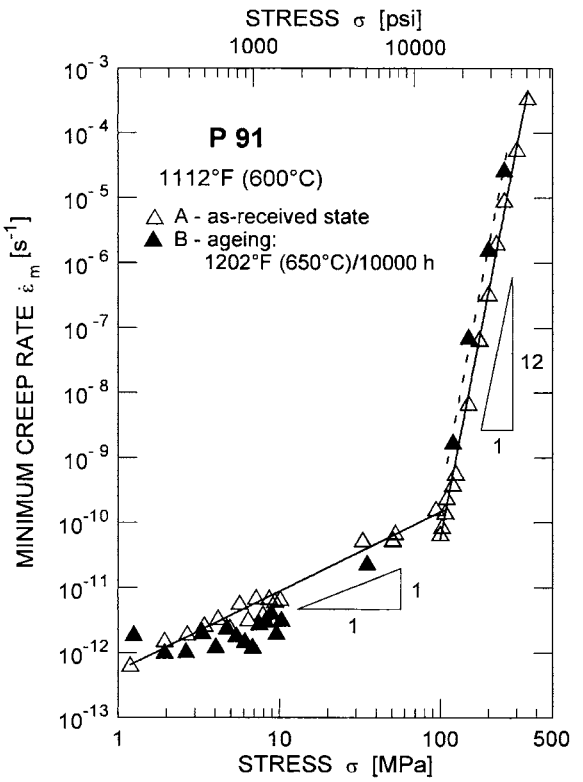

Figure 5. Stress dependence of minimum creep rate for P91 steel in power-law ($\sigma \geq 14500$ psi) and viscous ($\sigma < 14500$ psi) creep regimes.

Microstructural investigations

Microstructure of P91 steel is documented in Fig. 6. There are tiny precipitates of minor phase, present both on grain boundaries and on former martensitic laths, in as-received state, Fig. 6a. Isothermal annealing at 1202°F (650°C) for 10000 h leads to substantial coarsening of secondary phases particles on boundaries. Careful examination revealed also increase of very small particles inside the former martensitic laths, Fig. 6b. The similar situation was found out also for P92 steel, see micrographs in Fig.7. Nevertheless, stereological analysis of the crept specimens has revealed substantial difference between these two steels, mainly in number of particles in volume unit, after the creep exposure at 1112°F (600°C), as can be seen in Fig. 8. The isothermal annealing prior to creep test did not have any significant effect on number of particles in volume unit in P91 steel, as shown in Fig. 8a. By contrast, noticeable difference between the numbers of particles in volume unit for P92 steel was found in as-received and annealed state as shown in Fig. 8b.

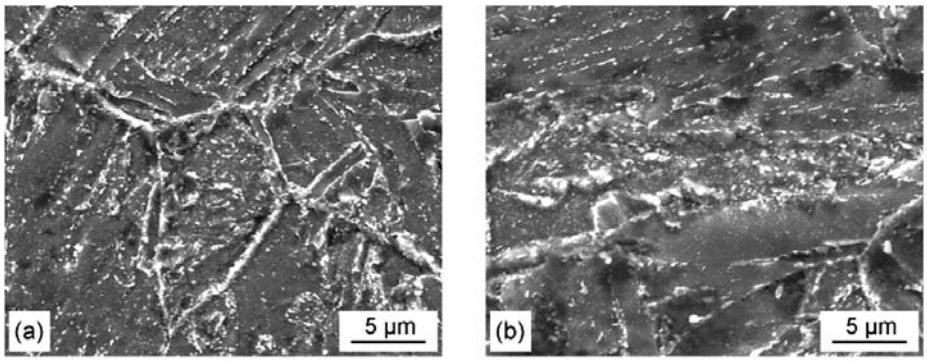

Figure 6. SEM micrographs showing microstructure of P91 steel: (a) in as-received state, and (b) after aging at 1202°F (650°C) for 10000 h

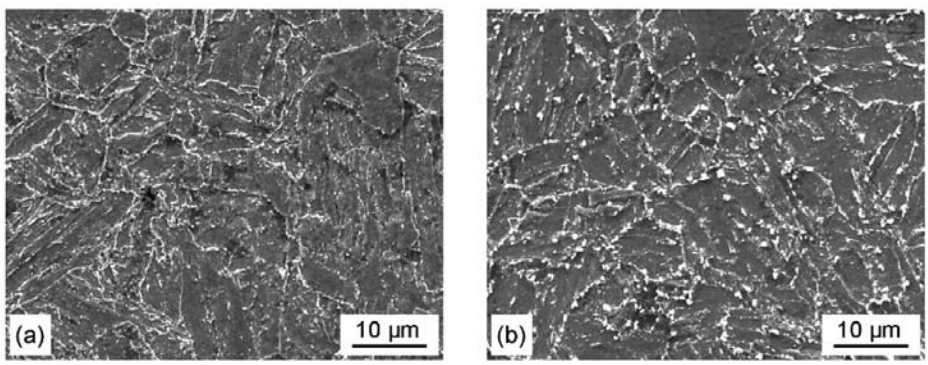

Figure 7. SEM micrographs showing microstructure of P92 steel: (a) in as-received state, and (b) after aging at 1202°F (650°C) for 10000 h

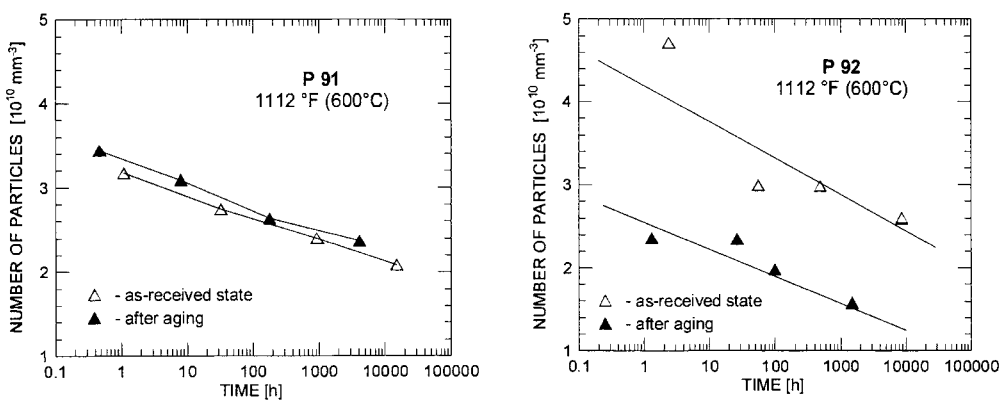

Figure 8. Time dependences of the volume density of particles for steels P91 and P92 crept at 1112°F (600°C) in as-received state, and after isothermal aging at 1202°F (650°C) for 10000 h prior to creep

Discussion

A power plant may have a life of 40 years. If a total creep strain of 1 pct is permissible, the average creep rate is about 10^{-11} s^{-1}. Extrapolation to this rate from rates measurable in the standard laboratory creep testing is perilous (Fig. 5), and we need to understand the physical processes involved. At these low rates of creep deformation the transport of matter occurs by migration of vacancies rather than by the glide of dislocations. These creep processes are usually classified as viscous creep [3,4]. Viscous creep can be proceeded by Nabarro-Herring and/or Coble diffusion creep or by Harper-Dorn creep. The existence and theoretical interpretation of viscous creep in pure metals are well established; by contrast, the understanding of viscous creep in materials hardened by precipitates is very incomplete at present.

At the lower stresses in Fig. 5, the experimental points appear to lie along a line having a slope of n = 1. It can be shown theoreticaly that there is a value of n = 1 for all viscous mechanisms. Thus, the low stress region of n = 1 in Fig. 5 can be attributed to viscous creep. However, it is less easy to distinguish experimentally between the occurence of Nabarro-Herring, Coble and/or Harper-Dorn creep giving the same value of n. The main difference between these mechanisms consists in the grain size dependence of the creep rate. Since the steel P91 of only one grain size was used, the present results do not provide any basis for the creep mechanisms identification.

Although no coherent explanation of the creep behaviour of the P91 steel in the low stress region (Fig.5) can be given along the mechanisms discussed above it can be concluded that no significant effect of microstructural stability on creep behaviour may be expected at low strain rates in which a regime of diffusion creep and/or Harper-Dorn creep dominates.

To determine the rate-controlling process(es) in creep in the high stress region $\sigma > 14500$ psi ($\sigma \geq 100$ MPa), the slopes of the minimum creep rates were determined at temperature of 1112°F (600°C) for both P91 and P92 steel in the as-received and aged states (Fig. 3a,b and Fig. 5). The stress dependence of the creep rate can be described by an equation of the power-law form:

$$\dot{\varepsilon}_{min} \alpha A\sigma^n$$

where A and n are constants at a given temperature. The observed high values of the stress exponent $n >> 1$ indicate the presence of the power-law or dislocation creep. The stress exponent n changes from 12 (steel P91, Fig. 3a and 5) to 18 (steel P92, Fig. 3b). Fig. 4 shows the stress dependence of the time to fracture t_f. Here again the straight-line approximation shows a good fit to the data, providing that the power-law relationship of the type

$$t_f \alpha B\sigma^{-m}$$

is obeyed. The observed values of the stress exponent m are very similar to the values for stress exponent n. This can be explained by the fact, that both the creep deformation and fracture are controlled by the same mechanism.

At present we are still some distance from a more complete description and understanding of significant microstructural features and deformation mechanisms responsible for the enhanced creep strength of tempered martensite ferritic 9-12%Cr steels in dislocation (power-law) creep. The movement of dislocations through the matrix is at first resisted by (a) the dislocation substructure distribution (dislocation strengthening mechanism), (b) intragranular particles, mainly MX (particle strengthening), and (c) the strain fields associated with elements in solid solution (solid solution strengthening). As creep progresses the dislocation substructure changes to form subgrains whose boundaries are stabilized by $M_{23}C_6$ and MX particles and possibly also by Laves phases. However, as these particles form and coarsen they denude the surrounding matrix of elements in solid solution, thus reducing the contribution of solid solution strengthening to creep resistance. Thus it seems likely that, as these changes progress, creep resistance becomes less and less dependent on resistance to the movement of individual dislocations through the matrix and more and more dependent on the resistance to subgrain growth through boundary migration.

Recently, Sklenicka et al [1] and Cadek et al [5] reported extensive studies and analyses of creep behaviour and microstructure of the P91 steel in the region of power-law creep. The analyses suggested strongly that (i) the creep rate is not recovery controlled, (ii) neither is the creep rate controlled by dislocation climb around carbide particles provided no interaction of dislocations with carbide particle takes place and finally (iii) the Rösler-Artz model assuming an attractive interaction of dislocations with dispersed particles and thermally activated detachment of the dislocations from the particles failed to account for the creep data of the P91. A metallographic analysis had shown that the effect of the rearrangement of dislocations and subgrain coarsening on creep may be more important than the effect of precipitation strengthening [1,6].

The contributions of the various microstructural features (dislocation density, subgrain size, carbide, carbonitride and intermetallic precipitates) to the creep strength of P92 steel were extensively studied [7]. Ennis [8] reported that in P92 steel, during the first 3000 h of exposure at 1112 – 1202°F (600 – 650°C) a rapid reduction in the dislocation density and increase in size of $M_{23}C_6$ precipitates occurs. The fine carbides, nitrides and carbonitrides are stable and do not coarsen significantly. Decreasing the dislocation density before testing by high temperature tempering reduces creep strength. If the martensitic transformation is suppressed by appropriate heat treatment, P92 steel exhibits very low creep strength. It is therefore important that an initial 100% martensitic microstructure is obtained. It should be stressed that the priority element having determined the original subgrain size and shape is the initial lath martensitic microstructure. Hattestrand and Andren [9] studied an isothermally aged P92 and found that coarsening of $M_{23}C_6$ carbides is accelerated by the strain, while the effect of strain on VN precipitates is insignificant. According to these authors MX (mainly VN) precipitates appear to be relatively stable at temperatures 1112°F (600°C) and 1202°F (650°C) up to 10000 h of ageing. With $M_{23}C_6$ precipitates the situation is different. At 1202°F (600°C), no coarsening appears to take place during 10000 h of ageing, while in creep the particles coarsen to about 20% larger size. At 1202°F (650°C) particle coarsening takes place in both aged and creep tested material. The role of tungsten (P92 steel has the addition of 1.8 wt% tungsten in comparison with

P91 steel) was studied by Hald [7]. It was found that W precipitates as intermetallic Laves phase during creep exposure, but the loss of tungsten from solid solution does not seem to affect long-term creep stability. Subgrains in steel P92 grow as a function of creep strain and stress following a general function for all 9-12%Cr steels, which indicates that the precipitate stability may control the creep strength of the steels. While MX (VN) particles coarsen very slowly during creep exposure, precipitation of new MX particles during creep could not be confirmed.

From the above discussion it can be concluded that the creep behaviour and creep strength in the power-law creep region are controlled by the coexistence of dislocation substructure and precipitates, the latter mainly acting as subgrain stabilizer. Thus, the role of dislocation substructure dominates the role of precipitation strengthening due to carbide particles. Consequently, a decrease of the creep resistance of the aged steels may be explained by taking account of the change of dislocation substructure during isothermal ageing.

The effect of nonsteady stressing and heating

Critical high temperature components of machines and structures are often subjected to complicated load and temperature histories. The closest laboratory simulation involves both the temperature and stress cycles. For example, the start up and shut down cycles can be well simulated by temperature cycling with or without hold times. Another type of nonsteady stressing is the isothermal loading with stress cycling. In order to consider the above effects of different loading, one needs to design experimental methods for simulating the operating state which has many cycles of heating/cooling and nonsteady stressing.

Nonsteady loading in power-law (dislocation) creep

As already described above, the power-law creep regime occurs in steel P91 at 1112°F (600°C) and applied stresses above 14500 psi (100 MPa) – Fig.5. No substantial difference in loading conditions inherent to the power-law creep can be expected for steel P92.

In this creep test, the specimens in one cycle were moved first from room temperature to 1112°F (600°C), then creep loaded (the holding time after stabilization of the temperature was 144 hours) and finally the specimens were cooled under load from 1112°F (600°C) to room temperature. This cycle was repeated from the beginning of the creep test up to the eventual fracture of specimen. Two creep curves with different loading history for steel P91 are shown in Fig. 9a in the form of strain ε versus time t for the testing temperature of 1112°F (600°C) and under the same level of the applied stress of 18125 psi (125 MPa). The first curve represents uninterrupted creep test which was run to the final fracture at constant temperature. The second curve shows the creep behavior of specimen with cycled temperature loading. This specimen was fractured after 66 cycles. The similar creep curves of steel P92 are shown in Fig. 9b for the same testing temperature and the applied stress of 21750 psi (150 MPa). In this case, the cycled specimen was fractured after 77 cycles.

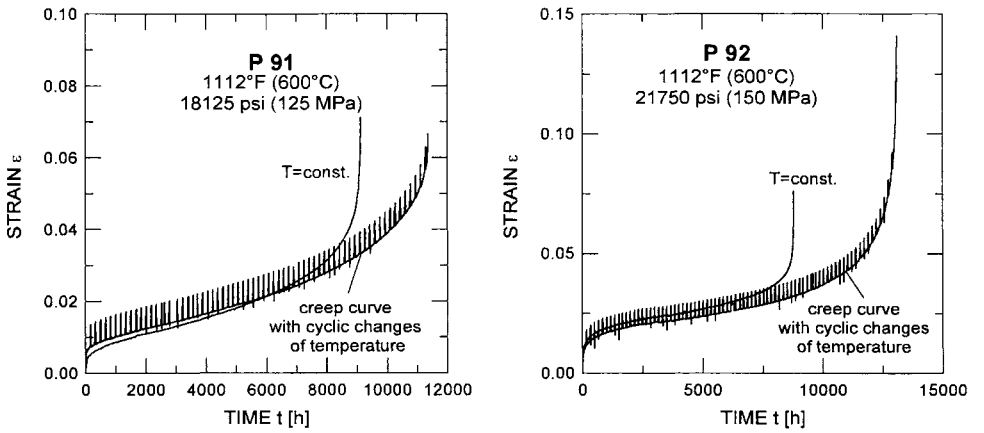

Figure 9. Creep tests with different loading history in power-law creep regime: (a) P91 steel, and (b) P92 steel

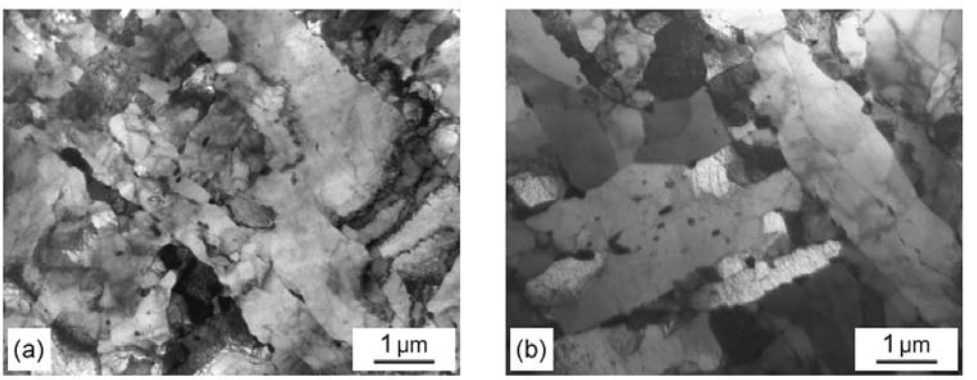

Figure 10. TEM micrographs of P91 steel subjected to monothonic creep: (a) gauge length, and (b) head part of creep specimen.

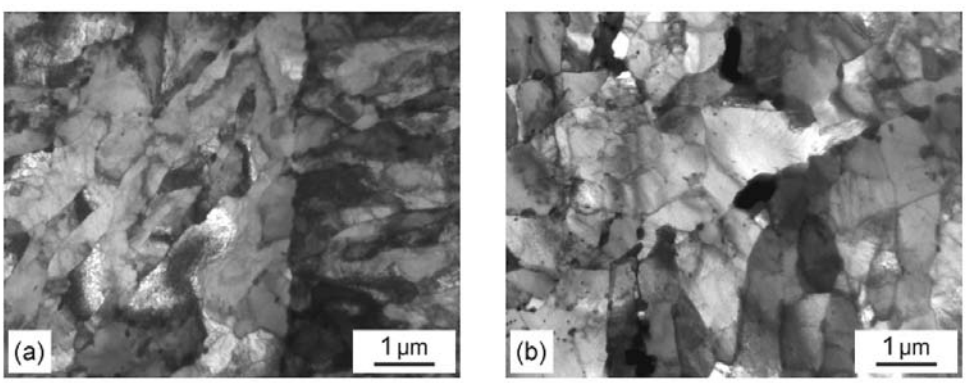

Figure 11. TEM micrographs of P92 steel subjected to monothonic creep: (a) gauge length, and (b) head part of creep specimen.

As demonstrated by the figures, no significant differences were found in the creep behaviour of the cycled tests when compared to the uninterrupted ones. The cycled specimens of steel P91 exhibit a little longer creep life then the uninterrupted specimens (Fig.9a). A possible explanation for this difference in creep life may lie in a serial addition of holding and cooling periods for a cycled specimen. In fact, the time to fracture for an uninterrupted specimen is about 9000 h whereas the test piece endurance for a cycled specimen is ~ 9500 h when derived from holding periods only. Thus, it is clear from these experiments that the creep life of steels P91 and P92 is not deteriorated by nonsteady heating.

The microstructures of specimens subjected to both the monotonic and nonsteady creep loading are very similar (Figs. 10 and 11) and exhibit an evolution that can be described by the following phenomena: (i) rearrangement and annihilation of excess transformation dislocations; the dislocation density decreases; (ii) equiaxed subgrains develop from the former tempered martensite structure. Dimensions of newly formed subgrains are finer in comparison to the former tempered martensite lath; (iii) interparticle spacing and size of carbides $M_{23}C_6$ and fine particles MX increase.

Nonsteady loading in viscous (low-stress) creep

Information on the mechanisms controlling creep deformation can be derived by monitoring the creep response to stress changes during a test. Such study of this type was carried out on steel P91 in the state after isothermal annealing at 1202°F (650°C) for 10000 h in the viscous creep regime. Creep test with the various load schedule were conducted at 1112°F (600°C) and the applied stress ranged from 5075 to 6380 psi (35 MPa to 44 MPa).

Some typical results are given in Fig. 12 showing the creep curves recorded in the stress change experiment. In this experiment, in which a specimen exposed for a period at an initial applied stress of 5075 psi (35 MPa), is then tested at a higher stress of 6380 psi (44 MPa) to reach the secondary creep stage. The stress is than reduced again from 6380 psi (44 MPa) to its original value of 5075 psi (35 MPa). This cycle is repeated several times during the experiment. For comparison of the transient effects in a creep test, the creep test at constant stress at 5075 psi (35 MPa) is included in Fig. 12. As demonstrated by the figure, significant differences were found in the creep behavior of the cycled and monotonic loaded specimens. Essentially, both the creep rate and the overal creep strain are higher in the constant stress experiments than in the stress change one. Some effect was observed on the creep behaviour of cycled specimens when the stress change experiment was interrupted, that is cooled down and after some time heated up to testing temperature again under constant load.

The details of creep curve during the temperature cycle are depicted in Fig. 13. There is also a transient effect, but much shorter than that of the stress change. The strain rate returns to its original value within approximately one day. Nevertheless, there is an additional strain after the interrupted which is not negligible.

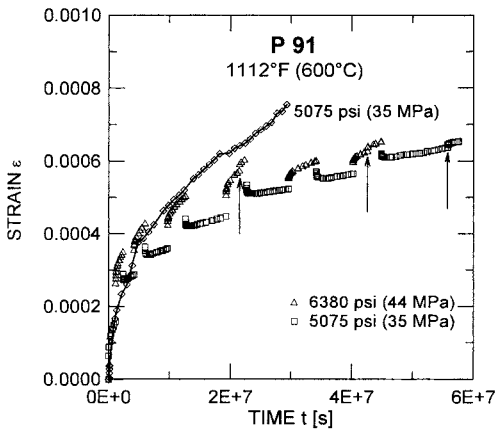

Figure 12. Creep curves recorded in the stress change tests of the P91 steel in viscous creep regime

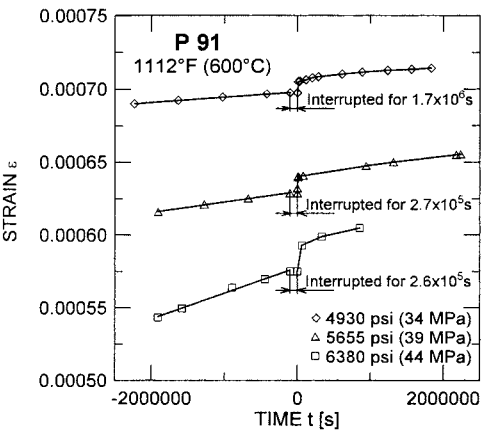

Figure 13. The details of the creep curves around the test interruption for the steel P91 at 1112°F and at the different levels of stress

Discussion

Interpretation of the detailed creep behavior following non-steady loading is not straightforward but several unambigous conclusions can be drawn. They should be based on the state of material, containing internal distribution of all microstructural elements, stress and strain. Since any of the state parameters may have its own kinetics depending on all other parameters, the solution of the problem is very difficult. It is important to realize that there is no physical reasons for conclusion, that every state of the material can be reached by loading history, like the combined constant stress constant temperature test.

Every stress change is followed by the transient stage resembling the primary stage of constant stress creep test, but the transient strain is negative after each stress decrease. This fact is fully

consistent with the results of Milicka and Dobes [10] indicating that the internal back stress is equivalent to the applied stress at stresses below about 20300 psi (140 MPa) for steel P91. The creep rate after the stress increase and decrease back to original value tends to reach considerably lower level than that obtained by the constant stress test. This indicates that some kind of strengthening occurs during the period of the higher stress. On the other hand, it is not possible to find any changes in the microstructure before and after creep test in viscous creep regime by the standard methods of the optical and electron metallography. This is not surprising, because the total strain reached in this type of experiment is too low to cause visible changes. In this situation, any conclusions concerning the strengthening mechanism could be only speculative. The creep rate starts to accelerate at the end of the constant stress creep test, while for stress change experiment remains more or less constant within longer time. This can be caused by some healing of the creep damage nuclei during the periods of negative creep flow. On the other hand, the structural development causing the decrease of the creep rate remains unclear. The positive influence of stress changes to the creep strength is consistent with the results of Vasina et al. [11]. They investigated the fatigue-creep interactions and found, that the small vibrations superposed on the creep test improve the creep strength of the steel when compared to the pure creep test.

The temperature changes consisting in cooling the specimen from the testing temperature of 1112°F (600°C) down to the room temperature and heating up again to the testing temperature may cause some additional strain generated by the thermal stresses created during temperature changes. However, this phenomenon seems to have no substantial effect on the creep behaviour of the specimen.

Conclusions

The creep resistance of two modified 9-12%Cr steels (grades P91 and P92) at 1112°F (600°C) is shown to be considerably influenced by microstructural changes during long-term aging at 1202°F (650°C) for 10000 h and/or creep over a range of dislocation (power-law) creep. By contrast, no significant effect of microstructural stability on creep was found in a regime of viscous creep at very low stresses. Further, no significant deterioration of the creep properties was found for the steel P91 under nonsteady loading in power-law creep in distinct from viscous creep regime.

Acknowledgements

Financial support for this work was provided by the Czech Science Foundation under Grant No 106/02/0608 (power-law creep experiments) and by the Academy of Sciences of the Czech Republic under Grants S2041001 and A2041101 (viscous creep experiments).

References

1. V. Sklenicka, K.Kucharova, A.Dlouhy and J. Krejci, "Creep Behaviour and Microstructure of a 9%Cr Steel", Proc. of Conference on Materials for Advanced Power Engineering, Liége, Belgium (October 1994), p.435.

2. L. Kloc, J. Fiala, and J. Cadek, "A New Procedure to Evaluate Creep Data Obtained by the Helicoid Spring Specimen Technique Under Conditions of Non-viscous Creep Behaviour", *Mater.Sci.Eng.,* A130, (1990), p.61.

3. Josef Cadek. *Creep in Metallic Materials.* Amsterdam, The Netherlands: Elsevier Science Publishers, 1988, pp. 205-234.

4. L. Kloc, V. Sklenicka, and J. Ventruba, "Comparison of Low Stress Creep Properties of Ferritic and Austenitic Creep Resistant Steels", *Mater.Sci.Eng.,* A319-321, (2001), p. 774.

5. J .Cadek, V. Sustek, and M. Pahutova, "An Analysis of Set of Creep Data for a 9Cr-1Mo-0.2V (P91) Steel", *Mater.Sci.Eng.,* A225, (1997), p.22.

6. A. Orlova, J.Bursik, K. Kucharova, and V. Sklenicka, "Microstructural Development During High Temperature Creep of 9%Cr Steel, *Mater. Sci. Eng.,* A245, (1998), p. 39.

7. J. Hald, "Microstructure Stability of Steels P92 and P122, Proc. Conference on Advances in Material Technology for Fossil Power Plant, Swansea, UK, (April 2001), p.115.

8. P. J. Ennis, et al. "Microstructural Stability and Creep Rupture Strength of the Martensitic Steel P92 for Advanced Power Plant", *Acta mater.,* 45, (1997), p. 4901.

9. M. Hattestrand, and H.-O. Andren, "Evaluation of Particle Size Distributions of Precipitates in a 9% Chromium Steel Using Energy Filtered TEM", *Micron,* 32, (2001), p.789.

10. K. Milicka, and F. Dobes, "Constant Structure Creep in a P91 Type Steel", *Engineering Mechanics*, 5, (1998), p. 165.

11. R. Vasina, P. Lukas, L. Kunz, and V. Sklenicka, "Interaction of High Cycle Fatigue and Creep in a 9%Cr-1%Mo Steel at Elevated Temperatures", *Fatigue Fract. Engng. Mater. Struct.,* 18, (1995), p. 27.